Effects of temperature on expansion of concrete due to the alkali-silica reaction: A simplified numerical approach

Y. Kawabata[a]✉, C. Dunant[b], S. Nakamura[a], K. Yamada[c], T. Kawakami[d]

a. Port and Airport Research Institute, (Yokosuka, Japan)
b. University of Cambridge, (Cambridge, U.K.)
c. National Institute for Environmental Studies, (Fukushima, Japan)
d. Kyushu University, (Fukuoka, Japan)
✉: kawabata-y@p.mpat.go.jp

ABSTRACT: The effects of temperature on the expansion behavior of concrete due to the alkali-silica reaction (ASR) were assessed through a simplified numerical analysis. Numerical models were constructed based on findings from a literature review. A simplified damage model was implemented to capture interactions between the viscoelasticity of the ASR gel and microstructural damage of the aggregate and paste. The parameters of the damage model were identified by fitting the simulated results to the experimental data. The results indicate that for a given reaction ratio, expansion ability is reduced at higher temperatures during the early and late stages of expansion. The results demonstrate that explicit modeling of chemo-mechanical interactions is important to achieve accurate numerical predictions of expansion behavior.

KEYWORDS: Temperature; Alkali-silica reaction; Expansion; Numerical simulation; Concrete prism test.

RESUMEN: *Efectos de la temperatura en la expansión del hormigón por la reacción álcali-sílice: una aproximación numérica simplificada.* Se evaluaron los efectos de la temperatura en el comportamiento expansivo del hormigón debido a la reacción álcali-sílice (ASR) mediante un análisis numérico simplificado. Los modelos numéricos se construyeron en base a la revisión de la literatura. Se implementó un modelo simplificado de daños para capturar las interacciones entre la viscoelsasticidad del gel (ASR) y el daño microestructural del árido y la pasta. Los parámetros del modelo de daños se identificaron mediante el ajuste de los resultados simulados a los datos experimentales. Los resultados indican que, para una determinada relación de reacción, la capacidad de expansión se reduce a temperaturas más altas durante las primeras y últimas etapas de la misma. Los resultados demuestran que la modelización explícita de las interacciones mecano-químicas es importante para conseguir predicciones numéricas precisas del comportamiento expansivo.

PALABRAS CLAVE: Temperatura; Reacción álcali-sílice; Expansión; Simulación numérica; Ensayo de prismas de hormigón.

This article was selected among the papers presented at the 2022 *International Conference on Alkali-Aggregate Reaction in Concrete* (16th ICAAR)

1. INTRODUCTION

Environmental conditions significantly affect the expansion behavior of concrete due to the alkali-silica reaction (ASR). Environmental factors include temperature, relative humidity (RH), solar insolation, and rainfall. These can cause temperature and moisture content to vary within the concrete, resulting in complex ASR expansion. The sensitivity of ASR expansion to temperature needs to be understood as temperature is a significant factor. Although several studies have investigated the influence of temperature on the expansion rate and final expansion (1–5), the relationship between the rate and sensitivities of expansion and final expansion to temperature remain unclear. For instance, according to Larive (6), temperature does not affect the final expansion, but it strongly affects expansion kinetics. Larive also reported that the dependency of ASR expansion kinetics on temperature conforms to Arrhenius's law. According to Kim et al. (7), the changes in the concentrations of alkali metal ions in the pore solution can be represented by a first order reaction. Also, expansions at different temperatures followed similar trends to the corresponding consumption of available alkalis. These findings indicate that the rate of ASR expansion is almost equivalent to reaction kinetics, but this was not shown by all studies. In some experiments, the final expansion was larger at lower temperatures (3–4), while others showed the pessimum effect of temperature on the final expansion (8–10).

It will be beneficial to model these expansion behaviors when coupled with the chemical reaction. In recent years, many chemo-mechanical models for micro- to mesoscopic ASR expansion have been developed (11–19). In the model by Dunant (11), expansion pressure comes from a phase change of the reactive silica from a dense and stiff mineral to a less dense and softer gel under confined conditions. On the other hand, in the model by Multon and Sellier (14), expansion pressure is not induced by the phase change. Rather, it is exerted after the ASR gel fills the pores in the paste and is calculated using the Biot coefficient. It is well known that temperature is a critical factor for the reaction and expansion, but its mechanisms are not well understood. The effects of temperature on ASR expansion may be strongly related to the mechanisms of pressure exertion by ASR gel.

In terms of micromechanics, ASR expansion induces microstructural damage on the aggregate and cement paste. In the early stages, expansion is mainly controlled by the reaction. In the later stages of the reaction, the reaction speed can interact with the formation of damaged structures. Reaction kinetics alone may be insufficient for predicting the expansion behavior due to ASR. Mechanical interactions are critical to the rate of concrete expansion and

have been discussed in (11). Expansion pressure exerted by the ASR gel inside reactive aggregates is a key factor in the swelling mechanism of concrete. Microcracks induced by the swelling of the ASR gel originate from the aggregate and extend to the cement paste. The crack patterns in the aggregate, such as onion skin and sharp cracks (20), are strongly dependent on the reactive rock type (19), and the random distribution of the expansion sites in the aggregate. The resulting damage to the microstructure alters mechanical response to expansion pressure (11–12). Creep of the paste also modifies the microstructural damage, as the degree of reaction at which the damage propagates from the aggregate to the paste is smaller with faster reaction kinetics (12). Therefore, the damage at a given reaction ratio is typically much greater in laboratory tests than in real structures due to creep. The activation energy of cement paste creep is 4.2–25.2 kJ/mol (21), whereas that of the dissolution rate of quartz glass and Pyrex glass is 63–84 kJ/mol (22). Therefore, high temperatures accelerate dissolution (almost equivalent to the reaction) more than creep. However, previous studies have shown complex behaviors at different temperatures (3–4, 8–10).

This paper is an extension of a previous paper (23) and investigates the effects of temperature on ASR expansion in concrete using a simplified numerical analysis. First, a brief literature review on the factors of the temperature dependence of ASR expansion is provided. Then, simplified models accounting for the temperature dependence of ASR expansion are presented. A damage model is implemented to represent the nonlinear relationships between reaction kinetics and expansion behavior. The parameters in the model are identified by fitting the simulated results to the experimental data. Finally, the effects of temperature on ASR expansion are discussed.

2. FACTORS AFFECTING TEMPERATURE DEPENDENCE OF ASR EXPANSION

Many factors affect the temperature dependence of ASR expansion, including the alkalinity of pore solution, internal RH, reactivity of aggregates, aggregate stiffness, strengths of paste and mortar, and viscosity of ASR gel. Higher temperatures reduce the pH of the pore solution as ettringite has higher solubility (24). Also, alkalinity is reduced where the alkalis leach out from laboratory specimens, which reduces ASR expansion. Less moisture is available for ASR expansion because internal RH is higher at higher temperatures (25). Generally, the temperature dependence of dissolution kinetics for amorphous silica in high pH solutions almost conforms to Arrhenius law (26), but this is not the case for some natural aggregates (27). The texture of the aggregate can strongly affect dissolution kinetics due to their

random distribution of silica minerals and paths for alkali transfer. It was reported that the reaction kinetics of some natural aggregates with dense microstructures could be changed with the reaction ratio (26, 27). Aggregate stiffness and paste strength are relatively important in the mechanical interaction, especially in the later stages when the reaction is advanced. If the ASR gel has low viscosity, it can flow out of the aggregate or concrete, while exerting reduced expansion pressure under confinement (28).

3. NUMERICAL MODELS

A simplified numerical simulation was proposed based on existing models (29), with an additional damage model accounting for the reduced expansion ability of ASR gel.

3.1 Alkalinity model

In the pore solution, alkali metal ions are generally balanced with hydroxide ions at a 1:1 ratio, so the alkalinity represents the alkali metal hydroxide concentration. Therefore, it is sufficient to only model the alkalinity of the solution. By considering the system as closed without any supply or leaching of alkali, the total amount of alkali (Na + K) per unit volume of mortar C_{mortar} can be expressed by the following equation from Kawabata et al. (30):

$$C_{mortar} = C_{cp}A_{cp} + C_{ag}A_{ag} + \gamma_{Na/Si}V_{gel}, \qquad [1]$$

where C_{cp} is the total alkali content per unit volume of cement paste (mol/m³-paste), A_{cp} is the cement paste content in the mortar (m³-paste/m³-mortar), C_{ag} is the alkali content instantaneously consumed by the aggregate (mol/g-aggregate), A_{ag} is the total reactive aggregate content in the mortar (g-aggregate/m³-mortar), $\gamma_{Na/Si}$ is the (Na+K)/Si molar ratio of the ASR gel, and V_{gel} is the total amount of ASR gel in the mortar (mol/m³-mortar). Note that the alkalis supplied from aggregates are not considered since alkalis do not necessarily increase the pH of the pore solution (31).

Considering the equilibrium between the solid C-S-H gel and pore solution in the cement paste system, C_{cp} may be written as:

$$C_{cp} = R_s C_{CSH} + R_l C_{fw}, \qquad [2]$$

where C_{CSH} is the amount of C-S-H per unit volume of cement paste (g/m³-paste), C_{fw} is the free water per unit volume of cement paste (ml/m³-paste), R_s is the alkali content in the solid C-S-H (mol/g), and R_l is the alkali concentration in solution (mol/mL). The distribution ratio, R_d (mL/g), may be described by the next Equations:

$$R_d = R_s/R_l \text{ and} \qquad [3]$$
$$R_d = \gamma(Ca/Si)^\delta, \qquad [4]$$

where Ca/Si is the Ca/Si molar ratio, and γ and δ are experimental constants, which were 2.5 and −3.1, respectively (30).

3.2 Reaction model

Following the work of Furusawa et al. (26), the reaction was modeled one-dimensionally from the surface of the aggregate towards the interior. Assuming that the alkali profile within the reaction layer is linear, the reaction ratio can be expressed as:

$$dx/dt = (C_{cp} - C_{th})k/x, \qquad [5]$$

where t is the duration of the reaction (hr), x is the thickness of the reaction layer (cm), k is the reaction rate constant (cm²/hr), C_{cp} is the concentration of alkali metal hydroxide in the paste (mol/L), and C_{th} is the threshold concentration of alkali metal hydroxide (mol/L).

The initial condition in which x is zero when t is zero gives:

$$x = \sqrt{2\,k \cdot t \cdot (C_{cp} - C_{th})}. \qquad [6]$$

Assuming that the aggregate particle is spherical and the particle is in contact with the pore solution, the reaction ratio of the aggregate i with radius R_i can be formulated as:

$$\alpha_i = 1 - (1 - x/R_i)^3, \qquad [7]$$

where R_i is the radius of the particle (cm) and α_i is the reaction ratio of the particle with radius R_i.

After calculating the reaction ratio for each particle of each particle size, the total amount of ASR gel is given by Equation [8]:

$$V_{gel} = A_{ag} \times \Sigma\, \alpha_i \beta_i, \qquad [8]$$

where β_i is the ratio of radius R_i to the total aggregate weight.

3.3 Expansion model

The stress σ_{ASR} imposed on the aggregates due to ASR gel formation can be described as:

$$\sigma_{ASR} = S_{gel}V_{gel} \times 1000, \qquad [9]$$

where σ_{ASR} is the stress on the aggregates (MPa for gel), and S_{gel} is the stiffness per mol of ASR gel in the mortar (GPa/mol/m³-mortar).

Since the elastic modulus of aggregate is large, the elastic deformation of aggregate before cracking is negligible and is thus assumed to be zero for simplification. When the stress is greater than the critical tensile stress of the aggregate, ASR gel formed in the aggregates start to expand the mortar, giving:

$$\varepsilon = <\sigma_{ASR} - \sigma_{cr}>^+ \times E_d/E_{agg}, \quad [10]$$

where ε is expansion of the mortar, σ_{cr} is the critical tensile stress for aggregates to be cracked (MPa), E_{agg} is a modulus of the damaged aggregate (GPa), E_d is a variable for the conversion of the stress imposed on the aggregates to the expansion of the mortar (-), and $<X>^+$ is the positive part of X.

Hence, when E_d is constant, ASR expansion is linearly related to the reaction ratio. However, this expansion is not realistic. Aggregate and paste are damaged by ASR expansion and this damage simultaneously reduces the restraints on the ASR gel with the increase in expansion. Therefore, the expansion pressure on the ASR gel is released and reaction kinetics no longer control the expansion. A damage model is introduced as a simplifying assumption that expresses the microstructural damage and resultant reduced expansion pressure of the ASR gel as:

$$E_d = E_0 \times \exp(-\omega \times <\alpha_i - \alpha_{th}>^+), \quad [11]$$

where α_{th} is the threshold expansion above which the viscoelasticity of the ASR gel dominates the expansion due to reduced confinement from damage, E_0 is the initial value without damage, and ω is a parameter representing the interaction between the rate of damage evolution and viscosity of ASR gel. Note that this is a simplified model to represent the above factors. The model assumes an exponential decline in the stiffness, although the aggregate or paste will split apart in reality. This is consistent with commonly used damage models.

4. EXPERIMENTS AND NUMERICAL SIMULATION

The models presented in Section 3 contain unknown parameters including S_{gel}, E_0, σ_{cr}, ω, and α_{th}, which are critical factors affecting concrete expansion. Therefore, the parameters were determined by fitting the simulated results to the experimental data (23, 32, 33). Then, the relationships between the parameters and temperature were assessed.

4.1 Materials and mix proportions

Ordinary Portland cement with an alkali content of 0.55 wt% was used as the reference material. Two reactive coarse aggregates were used for testing: a highly reactive andesite (designated "TO") with trydimite reactive phase, and andesite from a different source (designated "SI") containing cristobalite and volcanic glass as the reactive minerals. Both aggregates have caused ASR damage in real structures. Considering the proportional pessimum effect, the reactive aggregate proportion was 30 wt% for both reactive aggregates. For comparison, published data (highly reactive andesite "NT" from (34)) were also included. Pure limestone "LSG" was found to be a non-reactive coarse aggregate by various test methods such as CPT, the chemical method, mortar bar method, and field experiences. Non-reactive limestone sand "LSS" was also used. The properties of the aggregates are summarized in Table 1.

The mix proportions of the concrete specimens are summarized in Table 2. The water content was 160 kg/m³, water-to-cement ratio was 0.50, and air content was 4.5 %. This mixture is commonly used in Japan. The grading of aggregate was in accordance with JIS but not controlled precisely like RILEM or CSA. The total alkali content (Na_2O_{eq}) of concrete was boosted to 5.50 kg/m³ by adding NaOH solution to the mixing water.

4.2 Expansion test (Alkali-Wrapped Concrete Prism Test: AW-CPT)

AW-CPT was applied as an expansion test for the concrete specimens (75 × 75 × 250 mm³). The general protocols are nearly identical to those of RILEM AAR-3 (38 °C) and AAR-4 (60 °C). The only difference is that concrete specimens are wrapped in a wet cloth containing an alkaline solution (1.5 mol/L NaOH). After the concrete specimens were demolded, they were submerged in water for 30 mins. This short submersion process was used despite 3–4% of the alkali leaching from the concrete during this step (8).

The concrete specimen was then wrapped with a nonwoven polypropylene cloth containing 50 g of 1.50 mol/L NaOH solution, which approximated the alkali metal ion concentration of the pore solution of concrete with 5.50 kg-Na_2O_{eq}/m³ (30). The wet cloth was placed on top of a thin plastic film on a table. Then, the specimen was placed on top of the cloth, and the cloth and film were wrapped around the specimen. The cloth was secured by rubber bands to prevent detachment. Plastic film (or a plastic bag) was used to minimize alkaline solution losses from the cloth and to prevent it from drying. Three wrapped specimens were placed over water in storage containers, which were then placed in temperature-controlled chambers at 20, 40, or 60 °C.

To measure length changes, the storage container was placed in a room at 20 °C for one day to let the specimens cool. After cooling and carefully separating the cloth from the specimens, the length and weight of the specimens and the weight of the cloth were

Table 1. Aggregate properties of the test specimens (32).

	Density (SSD) (g/cm³)	Water absorption (%)	Expansion at 14 days (ASTM C 1260, %)	Chemical test (JIS A 1145)	
				Sc (mM)	Rc (mM)
TO	2.69	1.52	0.43	637	100
SI	2.62	1.59	0.26	447	170
LSG	2.71	0.22	-	-	-
LSS	2.63	1.74	-	-	-

Table 2. Mix proportions of the test specimens (32).

	W/C (%)	Air (%)	s/a (%)	Content per unit (kg/m³)				
				Water	Cement	LSS	TO/SI	LSG
TO	50.0	4.5	45.0	160	320	821	309	724
SI							306	724

measured. Ion-exchanged water was added after the measurements to keep the solution mass in the cloth at 50 g. Note that alkaline solution was not used as an additional water supply to avoid an excessive supply of alkali to the concrete specimen. This process was necessary to supply enough moisture for the ASR. The same cloths were used throughout the testing process.

4.3 Results

The AW-CPT results for different temperatures are presented in Figure 1. For the TO aggregate, the early-stage expansion was higher at a higher temperature. At 60 °C, the expansion appeared to plateau after 50 weeks. At 38 °C, although the initial expansion onset was later than at 60 °C, the expansion continued over time and exceeded that at 60 °C after 78 weeks. At 20 °C, the expansion began at 15 weeks and was almost linear with time. For the SI aggregate, the expansion rates at the early and late stages were higher at higher temperatures. However,

while the early-stage expansion rate at 38 °C was 42% of that at 60 °C, the late-stage expansion rate at 38 °C was 65% of that at 60 °C. Regarding chemical reaction kinetics, the expansivity of ASR gel reduced for late-stage expansions at high temperatures. The early- and late-stage expansion rates are summarized in Figure 2. Note that early-stage expansion is defined as expansions smaller than 0.15%, since the expansions showed strong nonlinearity above approximately 0.15%. Also, the published data from our previous study are plotted as "NT aggregate" in the figure. The early-stage expansion rates depended strongly on temperature, while late-stage rates were almost constant and irrespective of temperature. These trends are consistent with the previous study.

The experimental results suggest that the reduction in the expansivity of ASR gel may be pronounced at higher temperatures, which could be strongly affected by the aggregate through the location of gel pockets and aggregate texture. A numerical simulation is required to separate the chemical reaction from the expansion.
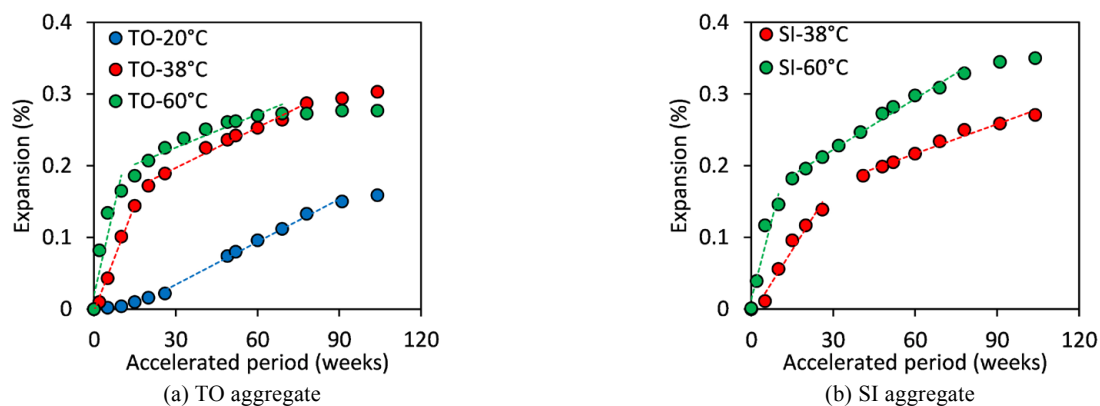

(a) TO aggregate

(b) SI aggregate

Figure 1. AW-CPT results at different test temperatures (32–33).
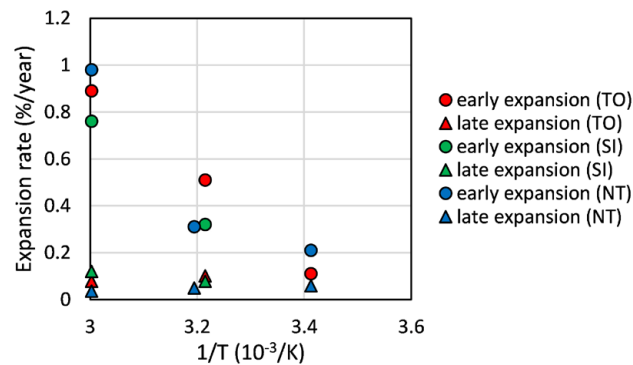
FIGURE 2. Temperature dependencies of the expansion rate with NT data from (34). The expansion rates were obtained from the dashed lines in Figure 1.

4.4 Numerical simulation and parameter identification

In the previous study (23), the parameters used in the damage model (ω and α_{th} in Eq. 11) were determined by fitting the numerical results to the experimental data. In this paper, the early-stage expansion rate was assumed to be a function of the stiffness of the gel (S_{gel}), and the late-stage expansion rate was a nonlinear parameter ω. The parameters were determined by fitting the numerical results to the experimental plots while fixing the other parameters for each aggregate.

The parameters (k, $\gamma_{Na/Si}$) of the reaction models and the activation energy of k were determined by chemical testing. Then, for the expansion models, σ_{cr} was determined from the expansion results for the TO aggregate at 20 °C. For $S_{gel} \times E_0$, the expansion results until 0.15% expansion for the TO aggregate at 38 °C were used. Above 0.15% expansion, ω was obtained to fit the late-stage expansion while fixing α_{th} for each aggregate. The same approach was applied to the SI and NT aggregates. Note that an early-stage expansion threshold of 0.05% was used for NT.

The results of the numerical simulation are presented in Figure 3. Temperature dependencies of the parameters are displayed as Arrhenius plots in Figure 4(a). Below 0.10–0.15% expansion, the calculated expansion curves were almost consistent with the experimental results, indicating that early-stage expansion almost conforms to reaction kinetics. In contrast, $S_{gel} \times E_0$ (representing early-stage expansion) depended strongly on temperature and reduced with increasing temperature. The activation energy was different for each aggregate type. This suggests that the stiffness of ASR gel can be reduced even in the early stage, and the effect of temperature on the stiffness varies with aggregate type.

For late-stage expansion, the numerical expansion curves were fitted to the experimental plots by changing ω. Note that according to our previous study, there were large discrepancies between the numerical and experimental results when ω was zero at expansions above 0.10–0.15%. This means that expansion behavior is not equivalent to reaction kinetics. Thus, late-stage expansion cannot be simulated by only considering the chemical reaction. Arrhenius plots of ω are shown in Figure 4(b). The parameter ω depended on temperature for TO and NT, but not for SI. This indicates that the reduction in the expansion ability of ASR gel varies for different aggregate characteristics such as reactive minerals and texture, which is strongly related to how ASR gel exerts expansion pressure inside the aggregate. For TO and NT, higher temperatures increased ω. This may indicate that excessively high temperatures cause considerable amounts of ASR gel to exude from the reaction site (gel pocket) and lose its expansion ability in the late stage.
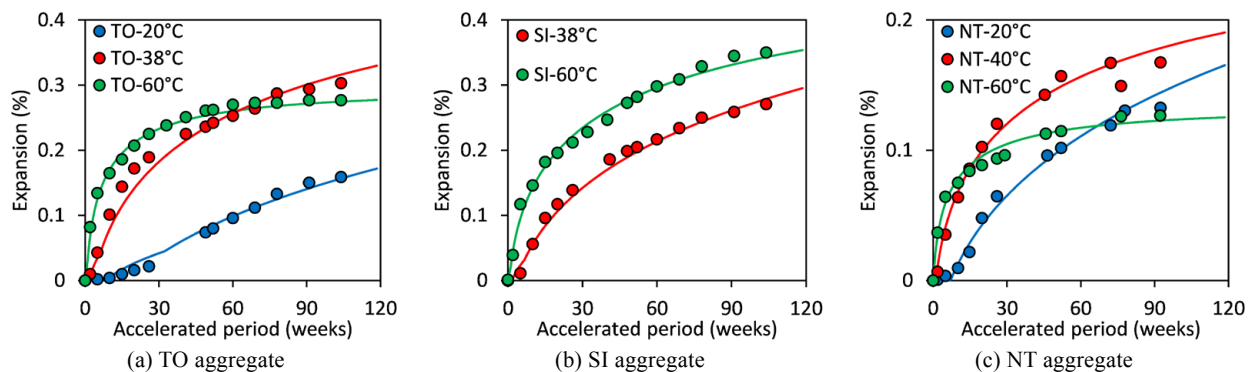

(a) TO aggregate

(b) SI aggregate

(c) NT aggregate

FIGURE 3. Results of the numerical simulation with and without the damage model.
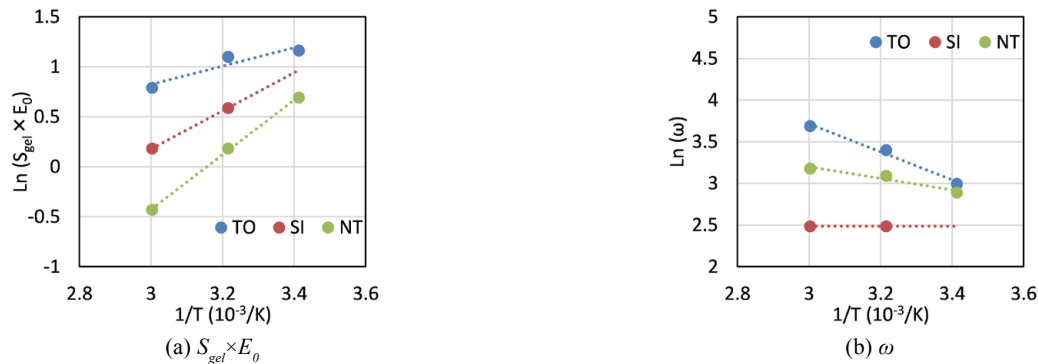
(a) $S_{gel} \times E_0$

(b) ω

FIGURE 4. Arrhenius plots of the parameters.

5. DISCUSSION

The simulation results were consistent with the experimental data when the damage model was implemented. Although early-stage expansion is mainly controlled by reaction kinetics, the damage process and viscoelastic behavior of the gel may be critical for expansion behavior. Reaction kinetics alone may be insufficient to assess the expansion behavior due to ASR.

The findings from the present study are consistent with the previous study (23), but some important issues are indicated. According to Dunant (11), the mechanisms of expansion and damage can be categorized into three stages: elastic expansion, aggregate failure, and paste cracking. Elastic expansion was assumed to be zero in this study. Therefore, expansion with quasi-brittle behavior until aggregate failure is attributed to early-stage expansion, while cracks in the aggregate extend to the paste during late-stage expansion.

The previous study reported that there was less damage and the ASR gel was well restrained in early-stage expansion, due to the low reaction ratio of the aggregate (23). Therefore, early-stage ASR expansion is less affected by viscoelasticity and microstructural damage. However, the re-assessment of the parameters in the present paper indicates that ASR gel may become less stiff, and a greater amount of ASR gel may not be responsible for expansion (possibly because it flows out of the confined system) even in the early stage, when the temperature is higher. Since damage is accumulated in the aggregate in early-stage expansion, some ASR gel may be lost for expansion. In the late stage, microcracks in the aggregate extend to the paste, which increases the complexity of expansion mechanisms. The parameter-fitting results indicate that the expansion ability of ASR gel is reduced at high temperatures. This means the rate of late-stage expansion is higher at lower temperatures at a given reaction ratio of the aggregate. Hence, the long-term expansion of concrete may be higher at lower temperatures. Previous studies attributed the reduced expansion at higher temperatures to reduced alkalinity related to ettringite solubility, enhanced alkali leaching, and less available moisture. Previous experiments showed that expansion can be reduced by a reduction in the expansion ability of ASR gel, due to modified ASR gel properties, and the interaction between aggregate and paste at higher temperatures. These findings are supported by our numerical approach.

According to Figure 4, the activation energy of $S_{gel} \times E_0$ was between 7.7 and 22.8 kJ/mol, and that of ω was between -5.8 and -14.0 kJ/mol. The value of $S_{gel} \times E_0$ was notably close to that of creep, compared to the higher value of dissolution. This may indicate that $S_{gel} \times E_0$ is dominated by creep. The negative activation energy of ω indicates that this parameter may be affected by other factors such as flow out of ASR gel due to microcracking.

The long-term expansion behavior of concrete with TO aggregate was simulated with different temperature histories (Figure 5). Long-term expansions at 20–30 °C reached or exceeded the plateaued expansion at 38 °C. Notably, the expansion for the case with a cyclic temperature history between 10–20 °C was slightly larger than that at 20 °C, which is the average cyclic temperature. Similar results were obtained in our previous study (35), in which concrete blocks (0.4 × 0.4 × 0.6 m) manufactured using the same aggregates at the same proportions were exposed to field conditions in Fukuoka (18.7 °C annual mean temperature), Okinawa (24.2 °C), and Monbetsu (7.6 °C). The onset of expansion occurred earlier with higher temperatures, as expansion was first observed in Okinawa, followed by Fukuoka and Monbetsu. However, the long-term (around 2 years) expansion of the block was about the same in Fukuoka and Okinawa. These observations may be explained by the simulated expansions in this paper. Furthermore, expansion behavior is also affected by moisture supply in addition to temperature, so moisture supply should be considered (1, 2, 35).

These results indicate that the nonlinear relationship between reaction kinetics and expansion behavior should be considered. Our damage model is a
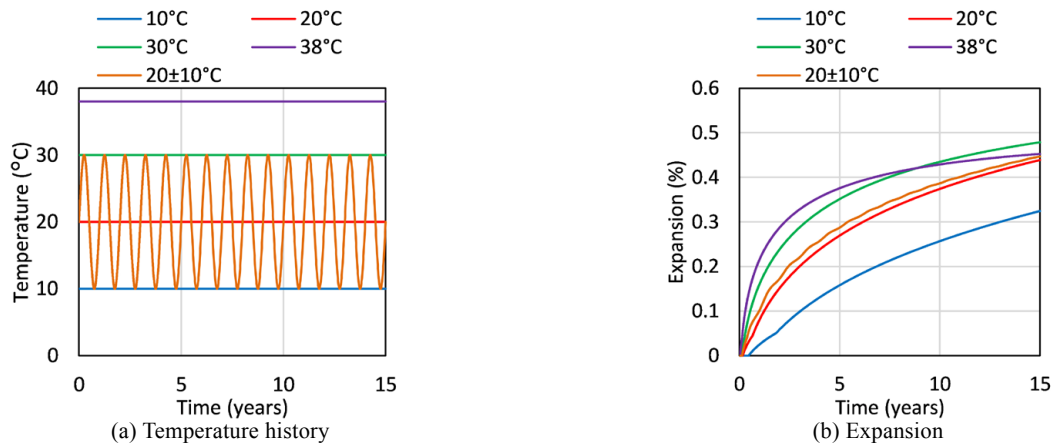
FIGURE 5. Simulated long-term behavior of concrete with TO aggregate.

simple way to address this, but the parameters differ between aggregate types. Therefore, further research is necessary to explore how parameters should be identified in terms of chemophysics.

6. CONCLUSIONS

The effects of temperature on the ASR expansion behavior of concrete were investigated using a simplified numerical approach. The parameters identified at different temperatures were compared. The conclusions are as follows:

– A simplified numerical simulation that considers chemical reaction kinetics and ASR gel expansion was presented. A simple damage model was implemented in the numerical framework to express a reduction in the expansion ability of ASR gel due to gel discharge from the sites.

– The parameters of the damage model were fitted to the experimental results. A reduction in the expansion ability during the early and late stages at higher temperatures was found. Therefore, this should be explicitly considered for more accurate modeling of ASR expansion at different temperatures.

– The activation energy of the parameters in the damage model differed between aggregate types. Although $S_{gel} \times E_0$ and the tested aggregate had similar general trends, the effect of temperature on ω is likely different for different aggregate types.

ACKNOWLEDGEMENTS

AUTHOR CONTRIBUTIONS:

Conceptualization: Y. Kawabata; Methodology: Y. Kawabata; Investigation: Y. Kawabata, C. Dunant, S. Nakamura, K. Yamada, T. Kawakami; Writing, original draft: Y. Kawabata; Writing, review & editing: C. Dunant, S. Nakamura, K. Yamada, T. Kawakami.

REFERENCES

1. Kawabata, Y.; Yamada, K.; Ogawa, S. (2017) Modeling of environmental conditions and their impact on the expansion of concrete affected by alkali-silica reaction. In: Sellier, Grimal, Multon and Bourdarot (ed), Swelling Concrete in Dams and Hydraulic Structures, Wiley, 163-175.
2. Kawabata, Y.; Yamada, K.; Ogawa, S.; Martin, R P.; Seignol, J F.; Toutlemonde, F. (2016) Correlation between laboratory expansion and field expansion of concrete: Prediction based on modified concrete expansion test. *Proc. of 15th Int. Conf. on Alkali-Aggregate Reaction*, 15ICAAR2016_034.
3. Fournier, B.; Ideker, J.H.; Folliard, K.J.; Thomas, M.D.A.; Nkinamubanzi, P.C.; Chvrier, R. (2009) Effect of environmental conditions on expansion in concrete due to alkali-silica reaction (ASR). *Mat. Charact.* 60 [7], 669-679. https://doi.org/10.1016/j.matchar.2008.12.018.
4. Lindgard, J.; Nixon, P.; Borchers, I.; Schouenborg, B.; Wigum, B.J.; Haugen, M.; Akesson, U. (2010) The EU "PARTNER" Project – European standard tests to prevent alkali reactions in aggregate: Final results and recommendations. *Cem. Concr. Res.* 40 [4], 611–635. https://doi.org/10.1016/j.cemconres.2009.09.004.
5. Ideker, J.H.; Drimalas, T.; Bentivegna, A.F.; Folliard, K.J.; Fournier, B.; Thomas, M.D.A.; Hooton, R.D.; Rogers, C.A. (2012) The importance of outdoor exposure site testing. *Proc. 14th Inter. Conf. Alkali-Aggregate Reac. Concr.* 051412-IDEK.
6. Larive, C. (1998) Apports Combinés de l'Expérimentation et de la Modélisation à la Compréhension de l'Alcali Reaction et de ses Effets Mécaniques Laboratoire Central des Ponts et Chaussées, OA28. (in French).
7. Kim, T.; Olek, J.; Jeong, H. (2015) Alkali-silica reaction: Kinetics of chemistry of pore solution and calcium hydroxide content in cementitious system. *Cem. Concr. Res.* 71, 36-45. https://doi.org/10.1016/j.cemconres.2015.01.017.
8. Kawabata, Y.; Yamada, K.; Ogawa, S.; Sagawa, Y. (2018) Alkali-Wrapped Concrete Prism Test (AW-CPT) – New testing protocol toward a performance test against alkali-silica reaction–. *J. Adv. Con. Tech.* 16 [9], 441–460. https://doi.org/10.3151/jact.16.441.

9. Swamy, R.S. (1991) The alkali-silica reaction in concrete, Blackie and Son Ltd.

10. Chatterji, S.; Christensen, P. (1990) Studies of alkali-silica reaction. Part 7. Modelling of expansion. *Cem. Concr. Res.* 20 [2], 285–290. https://doi.org/10.1016/0008-8846(90)90082-9.

11. Dunant, C.F. (2009) Experimental and modelling study of the alkali-silica-reaction in concrete, Ph.D thesis, École Polytechnique Fédérale de Lausanne.

12. Dunant, C.F.; Scrivener, K.L. (2010) Micro-mechanical modelling of alkali-silica-reaction-induced degradation using the AMIE framework. *Cem. Concr. Res.* 40 [4], 517–525. https://doi.org/10.1016/j.cemconres.2009.07.024.

13. Giorla, A.B.; Scrivener, K.L.; Dunant, C.F. (2015) Influence of visco-elasticity on the stress development induced by alkali-silica reaction. *Cem. Concr. Res.* 70, 1–8. https://doi.org/10.1016/j.cemconres.2014.09.006.

14. Multon, S.; Sellier, A. (2016) Multi-scale analysis of alkali–silica reaction (ASR): Impact of alkali leaching on scale effects affecting expansion tests. *Cem. Concr. Res.* 81, 122-123. https://doi.org/10.1016/j.cemconres.2015.12.007.

15. Yang, L.; Pathirage, M.; Su, H.; Alnaggar, M.; Luzio, G.D.; Cusatis, G. (2021) Computational modeling of temperature and relative humidity effects on concrete expansion due to alkali-silica reaction. *Cem. Concr. Compos.* 124, 104237. https://doi.org/10.1016/j.cemconcomp.2021.104237.

16. Takahashi, Y.; Ogawa, S.; Tanaka, Y.; Maekawa, K. (2016) Scale-dependent ASR expansion of concrete and its prediction coupled with silica gel generation and migration. *J. Adv. Con. Tech.* 14 [8], 444-463. https://doi.org/10.3151/jact.14.444.

17. Comby-Peyrot, I.; Bernard, F.; Bouchard, P.O.; Bay, F.; Garcia-Diaz, E. (2009) Development and validation of a 3D computational tool to describe concrete behaviour at mesoscale. Application to the alkali-silica reaction. *Comput. Mater. Sci.* 46 [4], 1163-1177. https://doi.org/10.1016/j.commatsci.2009.06.002.

18. Putatatsananon, W.; Saouma, V. (2013) Chemo-mechanical micromodel for alkali-silica reaction. *ACI Mater. J.*, 110, 67-77.

19. Miura, T.; Multon, S.; Kawabata, Y. (2021) Influence of the distribution of expansive sites in aggregates on the microscopic damage due to alkali-silica reaction (ASR) – insights into the mechanical origin of expansion–. *Cem. Concr. Res.* 142, 106355. https://doi.org/10.1016/j.cemconres.2021.106355.

20. Sanchez, L.F.M.; Fournier, B.; Jolin, M.; Duchesne, J. (2015) Reliable quantification of AAR damage through assessment of the Damage Rating Index (DRI). *Cem. Concr. Res.* 67, 74-92. https://doi.org/10.1016/j.cemconres.2014.08.002.

21. Kulug, P.; Wittman, F. (1969) Activation energy of creep of hardened cement paste. *Mate. Construc.* 2, 11-16. https://doi.org/10.1007/BF02473650.

22. Furusawa, Y.; Uomoto, T. (1993) A kinetics based evaluation to the effect of environmental factors on alkali-silica reaction. *JCA Pro. Cem. Concr.* 47, 402-407. (in Japanese).

23. Kawabata, Y.; Dunant, C.; Yamada, K.; Kawakami, T. (2021) Influence of temperature on expansion due to the alkali-silica reaction and numerical modelling, First Book of Proceedings of the 16th International Conference on Alkali-Aggregate Reaction in Concrete, 225-236.

24. Lothenbach, B.; Matschei, T.; Möschner, G.; Glasser, F.P. (2008) Thermodynamic modelling of the effect of temperature on the hydration and porosity of Portland cement. *Cem. Concr. Res.* 38 [1], 1–18. https://doi.org/10.1016/j.cemconres.2007.08.017.

25. Lindgård, J.; Sellevold, E.J.; Thomas, M.D.A.; Pedersen, B.; Justnes, H.; Rønning, T.F. (2013) Alkali–silica reaction (ASR) – performance testing Influence of specimen pre-treatment, exposure conditions and prism size on concrete porosity, moisture state and transport properties. *Cem. Concr. Res.* 53, 145–167. https://doi.org/10.1016/j.cemconres.2013.05.020.

26. Furusawa, Y.; Ohga, H.; Uomoto, T. (1994) An analytical study concerning prediction of concrete expansion due to Alkali-Silica Reaction. Proceedings of 3rd CANMET/ACI International Conference on Durability of Concrete, 757-779.

27. Kawakami, T.; Sagawa, Y.; Kawabata, Y.; Yamada, K.; Ogawa, S. (2021) A study on ASR expansion behavior of concrete exposed to natural environment for 5 years: Experimental and numerical approaches, In: Bridge Maintenance, Safety, Management, Life-Cycle Sustainability and Innovations – Yokota & Frangopol (eds), 2637-2643.

28. Kawabata, Y.; Yamada, K.; Ogawa, S.; Sagawa, Y. (2021) Mechanisms of internal swelling reactions: Recent advances and future research needs, In: Bridge Maintenance, Safety, Management, Life-Cycle Sustainability and Innovations – Yokota & Frangopol (eds), 2599-2607.

29. Kawabata, Y.; Yamada, K. (2017) The mechanism of limited inhibition by fly ash on expansion due to alkali-silica reaction at the pessimism proportion. *Cem. Concr. Res.* 92, 1-15. https://doi.org/10.1016/j.cemconres.2016.11.002.

30. Kawabata, Y.; Yamada, K. (2015) Evaluation of alkalinity of pore solution based on the phase composition of cement hydrates with supplementary cementitious materials and its relation to suppressing ASR expansion. *J. Adv. Con. Tech.* 13 [11], 538-553. https://doi.org/10.3151/jact.13.538.

31. Kawabata, Y.; Yamada, K.; Igarashi, G.; Sagawa, Y. (2018) Effects of solution type on alkali release from volcanic aggregates -Is alkali release really responsible for accelerating ASR expansion? *J. Adv. Con. Tech.* 16 [1], 61-74. https://doi.org/10.3151/jact.16.61.

32. Mitsubishi Research Institute, Inc. (2017) Project report of enhacing ageing management technical assessment FY2016 (Research on soundness evaluation of concrete structures in long term with respect to the Alkali Aggregate Reaction) (in Japanese).

33. Kawabata, Y.; Yamada, K.; Yanagawa, T.; Etoh, J. (2017) Modeling of ASR Expansion Behaviors of Concretes Tested by Accelerated Concrete Prism Test with Alkali-wrapping. Proceedings of the 12th JSMS Symposium on Concrete Structure Scenarios. 17, 491-496. (in Japanese).

34. Kawabata, Y.; Dunant, C.; Yamada, K.; Scrivever, K. (2019) Impact of temperature on expansive behavior of concrete with a highly reactive andesite due to the alkali-silica reaction. *Cem. Concr. Res.* 125, 105888. https://doi.org/10.1016/j.cemconres.2019.105888.

35. Kawabata, Y.; Yamada, K.; Ogawa, S.; Sagawa, Y. (2019) Numerical simulation of the expansion behavior of field-exposed concrete blocks based on a modified concrete prism test. Proceedings of International Conference on Sustainable Materials, Systems and Structures (SMSS 2019) Durability, monitoring and repair of structures, 230-237.